

Rhizaria in the oligotrophic exhibit clear temporal and vertical variability.

Alex Barth^{*1}, Leo Blanco-Berical², Rod Johnson³ and Joshua Stone¹

1. University of South Carolina, Biological Sciences, 700 Sumter St
401, Columbia, SC 29208
2. Arizona State University
3. Bermuda Institute of Ocean Sciences, Bermuda GE 01, UK

2 Introduction

3 Rhizaria are an extremely diverse super-group of single celled organisms consist-
4 ing of several phyla including retaria (foraminifera and radiolaria) and cercozoa.
5 These organisms exist in a wide range of habitats and are widely represented
6 in plankton communities throughout the global ocean. While the taxonomy of
7 these organisms has recently undergone several reclassifications (Biard, 2022a),
8 their presence in ocean ecosystems has been long known to oceanographers.
9 Some of the earliest records of their existence are from oceanographic expedi-
10 tions in the 19th century (Haekel, 1887). Rhizaria are unique members of the
11 plankton and protist community because they can reach large sizes (up to sev-
12 eral mm in diameter) and they construct intricate mineral skeletons out of either
13 silica, strontium, or calcium carbonate (Biard, 2022a; Kimoto, 2015; Nakamura
14 and Suzuki, 2015; Suzuki and Not, 2015). Despite their noticeable morphology
15 and global distribution, Rhizaria were largely understudied throughout the 20th
16 century. The bulk of modern plankton research has focused hard-bodied crus-
17 tacea which are numerically dominant and easily sampled with nets and preser-
18 vatives. Fragile organisms like Rhizaria, were difficult to adequately study as
19 they can be destroyed through standard zooplankton sampling techniques. A
20 number of studies in the late 1900s did employ alternative techniques to quantify
21 Rhizaria including diaphragm pumps (Michaels, 1988) or blue-water SCUBA col-
22 lections (Bijma et al., 1990; Caron et al., 1995; Caron and Be, 1984). However,
23 the bulk of Rhizaria research was constrained to sediment traps or paleontolog-
24 ical studies of sediment (Boltovskoy et al., 1993; Takahashi et al., 1983). Only

25 recently has the advent of molecular techniques and in-situ imaging tools ignited
26 a renewed focus on Rhizaria in pelagic ecosystems (Caron, 2016).

27 The wave of new data on Rhizaria has facilitated an improved understanding of
28 the significance in ocean ecosystem functions. Firstly, taxonomists have been
29 able to greatly refine the understanding of evolutionary relationships amongst
30 these diverse protists (Aurahs et al., 2009; Biard et al., 2015; Cavalier-Smith et
31 al., 2018; Decelle et al., 2013, 2012; rev by Biard, 2022a). DNA metabarcoding
32 studies have revealed insights into the distributional patterns Llopis Monferrer
33 et al. (2022), ecological relationships (Decelle et al., 2012; Nakamura et al.,
34 2023), and contribution to biogeochemical fluxes (Guidi et al., 2016; Gutierrez-
35 Rodriguez et al., 2019). Transcriptomic and proteomic approaches also have
36 been used to quantify rhizarian contribution to community metabolism (Cohen
37 et al., 2023). Yet, despite the excellent taxonomic resolution provided by molec-
38 ular approaches, they do not provide a truly quantitative metric for estimating
39 Rhizarian abundance or biomass. In-situ imaging tools however, offer the ability
40 to observe organisms in the natural state and quantify their abundance (Barth
41 and Stone, in review; Ohman, 2019). While there were early applicaitons of
42 imaging tools to document Rhizaria (Dennett et al., 2002), Biard et al. (2016)'s
43 report from a global imaging dataset highlighted the importance of Rhizaria to
44 the total standing stock of marine carbon. Due to their large sizes, ability to con-
45 centrate smaller particles (ballasting), and the unique structure of their mineral
46 skeletons, Rhizaria have the potential to massively influence ocean biogeochem-
47 ical cycling. A number of studies have made large advances in estimating the

48 contribution of Rhizaria to ocean cycling of carbon (Gutierrez-Rodriguez et al.,
49 2019; Ikenoue et al., 2019; Lampitt et al., 2009; Stukel et al., 2018), silica (Biard
50 et al., 2018; Llopis Monferrer et al., 2021), and strontium (Decelle et al., 2013).
51 Still, Rhizarian ecological roles are not well understood (Biard, 2022a). This is
52 a major challenge as it is critical to understand the ecological role of plankton
53 to fully incorporate them into biological oceanographic models.

54 The ecological role of Rhizaria in plankton communities is complicated due to
55 the fact different taxa can exhibit every different trophic modes. As zooplank-
56 ton, rhizaria are predominately heterotrophic (Biard, 2022a), yet their feeding
57 modes can be quite varied. Phaeodarians (family Cercozoa) are largely thought
58 to be flux-feeders, collecting and feeding on sinking particles (Nakamura and
59 Suzuki, 2015; Stukel et al., 2019). Alternatively, Retaria can be either exclu-
60 sively heterotrophic or mixotrophic, utilizing photosynthetic algal symbionts
61 (Anderson, 2014; Decelle et al., 2015). Mixotrophic foraminifera host a variety
62 of endosymbiont partners (Decelle et al., 2015; Lee, 2006), which are thought to
63 support early and adult life stages and contribute to total primary productivity
64 (Kimoto, 2015). Still, foraminifera are omnivorous, possibly even predominately
65 carnivorous with several studies suggesting that they can be effective predators
66 (Anderson and Bé, 1976; Gaskell et al., 2019), majoritively consuming live cope-
67 pods (Caron and Be, 1984). Radiolaria have several lineages all which have
68 some taxa who are well known to host symbionts (Biard, 2022b). Amongst radi-
69 olarians, arguably the most widespread are Collodaria who can be either large
70 solitary cells or form massive colonies, up to several meters in length (Swan-

71 berg and Anderson, 1981). All known Collodaria species host dinoflagellate
72 symbionts (Biard, 2022b) and can contribute substantially to primary produc-
73 tivity, particularly in oligotrophic ocean regions (Caron et al., 1995; Dennett
74 et al., 2002). This Collodaria-symbiont association has been suggested as a
75 reason for their high abundances throughout the photic zone of oligotrophic en-
76 vironments globally (Biard et al., 2017, 2016). A few Acantharean (Radiolarian
77 order) clades host algal symbionts (Biard, 2022b; Decelle et al., 2012), notably
78 with two clades forming an exclusive relationship with Phaeocystis. However,
79 globally Acantharea are less abundant than Collodaria (Biard, 2022a) and con-
80 tribute less to total primary productivity (Michaels et al., 1995). This may be
81 due to the fact several clades of Acantharea are cyst-forming and strictly het-
82 erotrophs (Biard, 2022b; Decelle et al., 2013). Furthermore, Mars Brisbin et al.
83 (2020) documented apparent predation behavior in Acantharea near the surface,
84 suggesting that there may be a large reliance on carnivory.

85 Given the high abundances, yet diverse trophic strategies found among Rhizar-
86 ian taxa, it is reasonable to expect some form of niche partitioning. A number
87 of studies do suggest evidence for vertical zonation between Rhizaria groups
88 according to various trophic strategies. Taxa-specific studies of radiolarians sug-
89 gest they may be restricted to the euphotic zone (Boltovskoy, 2017; Michaels,
90 1988). Although some studies report Acantharea in deeper waters (Decelle et
91 al., 2013; Gutiérrez-Rodríguez et al., 2022). Phaeodarians alternatively, are
92 generally found in the mesopelagic where photosynthesis cannot occur but they
93 can feed on sinking particles (Stukel et al., 2018). In an imaging-based study of

94 the whole Rhizaria community, Biard and Ohman (2020) noted clear patterns
95 in vertical zonation which largely corresponded to different trophic roles. In
96 the oligotrophic ocean, Blanco-Bercial et al. (2022) also noted that the protist
97 community, including Rhizaria partition along an autotroph and mixotroph to
98 heterotroph gradient with increasing depth in the water column. Yet, few stud-
99 ies have made direct attempts to relate rhizaria abundances to environmental
100 factors (Biard and Ohman, 2020). In part, this is due to the fact few stud-
101 ies have been able to sample Rhizaria in the same location over a consistent
102 timeframe (Boltovskoy et al., 1993; Gutiérrez-Rodríguez et al., 2022; Hull et
103 al., 2011; Michaels et al., 1995; Michaels, 1988). Furthermore, no studies have
104 utilized imaging, arguably the best method for quantifying rhizaria, consistently
105 throughout the full mesopelagic. Given this lack of information, there are many
106 unknowns with respect to Rhizarian ecology, seasonality and phenology across
107 different groups.

108 In this study, we present a comprehensive assessment of large Rhizaria measured
109 for multiple months (greater than 1 year) using an in-situ imaging approach.
110 With this dataset, we address two critical aims. 1) Quantification of large
111 Rhizaria throughout the epipelagic (0-200m) and mesopelagic (200-1000m) over
112 the course of an annual cycle. These data were collected in the Sargasso Sea,
113 and represents the first study of its kind in an oligotrophic system. 2) We aim to
114 test the hypothesis that Rhizaria exhibit niche partitioning according to trophic
115 roles. This hypothesis makes several predictions, including vertical zonation, as
116 seen in prior studies, but also that environmental variables related to trophic

¹¹⁷ strategy will explain abundance patterns. Specifically, autotrophic/mixotrophic
¹¹⁸ taxa will correspond to variables related to autotrophy (chl-a concentration,
¹¹⁹ primary productivity, high O_2) and other rhizaria will correspond to factors
¹²⁰ which promote heterotrophy (particle concentration, flux, and low O_2).

¹²¹ Methods

¹²² Oceanographic Sampling

¹²³ Data were collected in collaboration with the Bermuda Atlantic Time-Series
¹²⁴ Study (Lomas et al., 2013; Michaels and Knap, 1996) on board the R/V
¹²⁵ Atlantic Explorer. Cruises were conducted at approximately monthly intervals.
¹²⁶ Rhizaria individuals were sampled using the Underwater Vision Profiler 5
¹²⁷ [UVP5; Picheral et al. (2010)], a tool which is well established to accurately
¹²⁸ quantify large Rhizaria (Barth and Stone, 2022; Biard et al., 2016; Biard and
¹²⁹ Ohman, 2020; Drago et al., 2022; Llopis Monferrer et al., 2022; Panaiotis et
¹³⁰ al., 2023; Stukel et al., 2019; Stukel et al., 2018). The UVP5 was mounted
¹³¹ to the sampling rosette and collected data autonomously on routine casts,
¹³² from which only the downcast data are utilized. The UVP5 was deployed
¹³³ from June-September 2019 then from October 2020 - January 2022. Casts
¹³⁴ were filtered to only include data collected in the BATS region, far offshore
¹³⁵ of Bermuda into the Sargasso Sea (Supplemental Figure 1). In general, casts
¹³⁶ extended to either 200m, 500m, or 1200m deep, with a few extended into the
¹³⁷ bathypelagic (4500m). However, Rhizaria were only typically found in large

¹³⁸ abundances throughout the epipelagic and mesopelagic zones. As such, we
¹³⁹ limit this study to results from the upper 1000m of the water column.

¹⁴⁰ A variety of biotic and abiotic data were collected during each BATS cruise.
¹⁴¹ Briefly, we will explain the data utilized in this study. The UVP5 provided
¹⁴² particle count data at a high-frequency from each cast. Particle concentra-
¹⁴³ tion was calculated from this data for all particles $184\mu m - 450\mu m$. The lower
¹⁴⁴ size range was set by what could be reliably sampled by the UVP5's pixel res-
¹⁴⁵ olution ($>2px$) and the upper size range is representative of a potential prey
¹⁴⁶ field for mesozooplankton (Whitmore and Ohman, 2021). Salinity, temperature,
¹⁴⁷ Dissolved Oxygen (DO), and in-situ chlorophyll fluorescence were measured at
¹⁴⁸ high-frequencies on each cast, attached to the same CTD rosette as the UVP. On
¹⁴⁹ certain casts, niskin bottles were used to collect bacterial abundance estimates
¹⁵⁰ (via epifluorescence microscopy) as well as measure inorganic nutrients (NO_3 ,
¹⁵¹ and Si as silicate/silicic acid) at discrete depths. On each cruise, flux estimates
¹⁵² of total mass, carbon, and nitrogen were also collected using sediment traps (in
¹⁵³ the present study we utilize flux to the mesopelagic as the flux at 200m). Also
¹⁵⁴ primary productivity was estimated through measuring C^{14} uptake rates from
¹⁵⁵ in-situ incubations. Full descriptions of the BATS sampling program, methods,
¹⁵⁶ and data are available freely online (<https://bats.bios.asu.edu/bats-data/>) and
¹⁵⁷ reviewed in (Lomas et al., 2013).

¹⁵⁸ Environmental data were processed in a variety of ways to match the format
¹⁵⁹ of the Rhizaria abundance estimates (See below). CTD data were collected at
¹⁶⁰ higher frequency than the UVP, so these data were averaged within matching

¹⁶¹ bins to the UVP5 data. Data from niskin bottles were first linearly interpolated
¹⁶² with a 1m resolution for each cast where data were available. Then, because data
¹⁶³ were collected at different frequencies over the course of a cruise, the interpo-
¹⁶⁴ lated data were averaged across casts, then averaged into matching UVP5-sized
¹⁶⁵ bins. Primary productivity estimates were totaled within the euphotic zone to
¹⁶⁶ represent a “total euphotic productivity”. Finally the data from the sediment
¹⁶⁷ trap deployed to 200m was used to represent “flux to the mesopelagic”.

¹⁶⁸ Rhizaria imaging processing and quantification

¹⁶⁹ Individual vignettes of Rhizaria images were identified using the classification
¹⁷⁰ platform Ecotaxa [cite]. Data were pre-sorted according to a . Taxonomic
¹⁷¹ classification were done based on morphology exclusively. While there are
¹⁷² sparse taxonomic guides for in-situ images of rhizaria, identification largely
¹⁷³ relied on descriptions in (Nakamura and Suzuki, 2015; Suzuki and Not,
¹⁷⁴ 2015; and Biard and Ohman, 2020). Using the aforementioned sources and
¹⁷⁵ publicly available ecotaxa projects, I constructed a guide which can be found
¹⁷⁶ here: https://thealexbarth.github.io/media//Project_Items/Oligotrophic_Community/ecotaxa_UVP-guide-stone-lab.pdf. Broadly, Rhizaria were classi-
¹⁷⁷ fied as Foraminifera, Radiolarians (Acantharea or Collodaria), or a variety of
¹⁷⁸ Phaeodarian families (Figure 1). When identification could not be confidently
¹⁷⁹ made between a few candidate taxa, a less specific label was used. As a result,
¹⁸⁰ we have data from “unidentified Rhizaria”, which typically were vignettes
¹⁸¹ not distinguishable between Aulacanthidae or Acantharea or “unidentified

¹⁸³ Phaeodaria”, which are clearly phaeodaria but not distinguishable into a
¹⁸⁴ family.

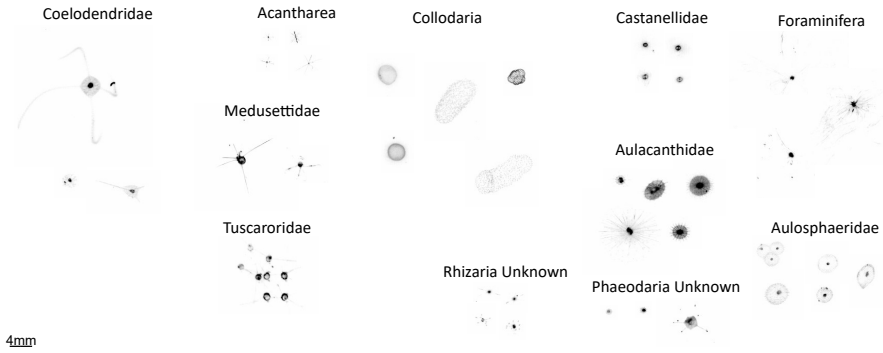


Figure 1: Example images of different Rhizaria taxa. 4mm scale bar shown in lower right. All vignettes are same scale

¹⁸⁵ The UVP5 samples at ~15Hz rate as it descends the water column and records
¹⁸⁶ the exact position of each particle larger than $600\mu m$. However, identified
¹⁸⁷ rhizaria ranged from a $934\mu m$ Aulacanthidae cell to a Collodarian colony over
¹⁸⁸ 10mm in diameter. To confirm that the UVP5 was sampling adequately across
¹⁸⁹ all size ranges, an NBSS slope was constructed to identify a drop-off which
¹⁹⁰ would indicate poor-sampling at the small size range (Barth and Stone, in
¹⁹¹ review; Lombard et al., 2019) . However, it was evident from this analysis
¹⁹² that all size ranges were adequately sampled across the size range (Supplemen-
¹⁹³ tal Figure 2) so no data were excluded. The UVP5 reports the exact depth
¹⁹⁴ at which a particle is recorded, however to estimate abundance, observations
¹⁹⁵ must be binned over fixed depth intervals. In our deployments had variable
¹⁹⁶ descent depths and speeds with more casts descending to 500m than 1000m
¹⁹⁷ and descents quicker through the epipelagic than the mesopelagic [see Barth

and Stone (2022) for an extended discussion of UVP5 data processing). For the present study, Rhizarian abundances were estimated in 25m vertical bins, which offer a moderate sampling volume (average $0.948m^3$ in the epipelagic and $0.589m^3$ in the mesopelagic) while still maintaining ecologically relevant widths. However, concentrations in a 25m bin would need to be greater than 2.428 indv. m^{-3} and 3.912 indv. m^{-3} , in the epipelagic and mesopelagic respectively, to fall below a 10% non-detection risk (Barth and Stone, in review; Benfield et al., 1996). Because we typically observed many rhizaria taxa below these concentrations, we present the 25m binned data to visualize broad-scale average distributions. For quantifying and modelling Rhizaria abundances, we present integrated abundance estimates, with each cast. Due to the variable descent depths of the UVP, data are categorized as epipelagic (0-200m), upper mesopelagic (200-500m), and lower mesopelagic (500-1000m). The average sampling volume integrated through these regions were $7.59m^2$, $7.06m^2$, and $11.77m^2$, with non-detection thresholds at 0.30 indv. m^{-2} , 0.33 indv. m^{-2} , and 0.20 indv. m^{-2} respectively. All UVP data processing was done using the EcotaxaTools package in R (Barth 2023).

Modelling environmental controls of Rhizarian Abundance

Generalized Additive Models (GAMs) were used to assess the relationship between integrated Rhizarian abundance and different environmental factors. GAMs offer the ability to model non-linear and non-monotonic relationships, which can be particularly useful in assessing ecological relationships (Wood,

²²⁰ 2017) and have been successfully applied to Rhizarian ecology (Biard and
²²¹ Ohman, 2020). The `mgcv` package (Wood, 2001) was used to construct models
²²² relating environmental parameters to each taxonomic group's integrated
²²³ abundance estimates from each cast. To select the most parsimonious model
²²⁴ for each analysis, a backwards step-wise approach was taken. First, a full
²²⁵ model was fit using any term which may be ecologically relevant. Terms were
²²⁶ fit using maximum likelihood with a double penalty approach on unnecessary
²²⁷ smooths (Marra and Wood, 2011). The smoothness parameter was restricted
²²⁸ ($k = 6$) to prevent overfitting the models. At each iteration of the backwards
²²⁹ step-wise procedure, the model term with the lowest F score (least statistically
²³⁰ significant) was removed. This was repeated until all model terms were
²³¹ statistically significant or the R^2_{adj} was substantially reduced. Models were fit
²³² for each region; epipelagic, upper mesopelagic, and lower mesopelagic. In cases
²³³ where observations were too sparse for a given taxonomic grouping, models
²³⁴ were not run.

²³⁵ Results

²³⁶ Environmental Variability

²³⁷ The BATS sampling region is southeast of Bermuda, situated in the North Sar-
²³⁸ gasso Sea and the North Atlantic oligotrophic ocean gyre. Due to the sampling
²³⁹ location, while the environmental conditions are generally low in variation and
²⁴⁰ oligotrophic, there is some seasonality and considerable influence from mesoscale

²⁴¹ eddies (Lomas et al., 2013; McGillicuddy et al., 1998). Variability in the wa-
²⁴² ter column structure was visible during the study period (Figure 2). This is
²⁴³ best evidenced through the temperature profiles; In the late summer and early
²⁴⁴ fall there was a stratified water column with high temperatures in the surface
²⁴⁵ (<75m) (Figure 2A) and slightly elevated salinity (Figure 2B). This warm, strat-
²⁴⁶ ified period appeared more intense during the few months sampled in 2019. In
²⁴⁷ 2021, we observed the stratified layer slowly dissipated into the winter months.
²⁴⁸ There was a consistent oxygen minimum zone (OMZ) located at about 750m
²⁴⁹ deep (Figure 2C). Although, February 2021 saw a notable downwelling event,
²⁵⁰ likely due to a passing cyclonic eddy. During this time, warmer, oxic water was
²⁵¹ plunged deeper into the mesopelagic. This process was reversed in the spring
²⁵² months (March, April) when mixing occurred throughout the epipelagic and the
²⁵³ surface was cooler and well mixed. Primary production was highest during the
²⁵⁴ spring mixing period, evidenced both by in-situ fluorescence (Figure 2D) and
²⁵⁵ productivity incubation experiments (Figure 3A). Originating near the surface,
²⁵⁶ the productivity peak moved deeper throughout the spring and declined into
²⁵⁷ the summer (Figure 2D). However, there was a notable, yet smaller productiv-
²⁵⁸ ity bump in the late summer and early fall (Figure 3A) which occurred deeper
²⁵⁹ in the epipelagic (Figure 2D). The particle concentration ($184\mu m - 450\mu m$) was
²⁶⁰ closely coupled to chlorophyll-a patterns.

²⁶¹ Overall, particle concentration was high near the surface during the 2021 spring
²⁶² bloom, then sank throughout the water column attenuating throughout the
²⁶³ lower epipelagic (Figure 2E). Similarly, bacteria abundance was closely linked

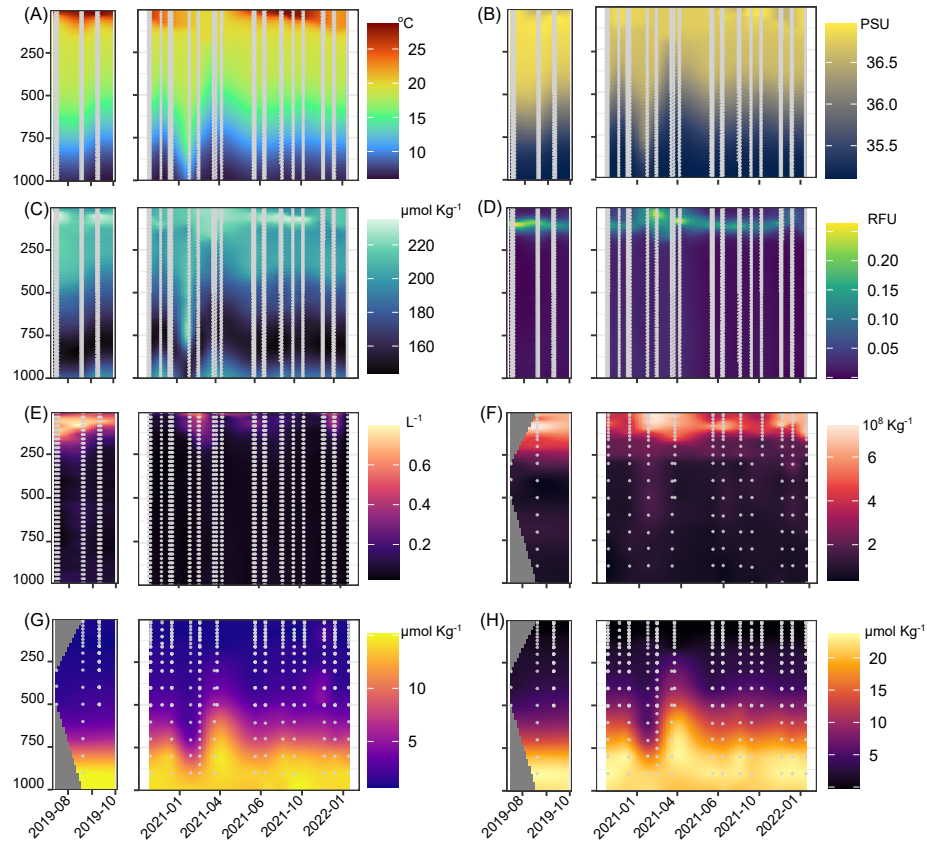


Figure 2: Environmental profiles across time-series of study period. Y axis shows depth in meters. (A) Temperature. (B) Salinity. (C) Dissolved Oxygen. (D) In-situ chlorophyll fluorescence. (E) Particle concentration ($184 - 450 \mu\text{m}$). (F) Bacteria Abundance. (G) Silica. (H) Nitrate

²⁶⁴ to overall productivity, although there was a more consistent layer near the
²⁶⁵ top of the mesopelagic (~250m) (Figure 2F). Concurrent with the secondary
²⁶⁶ fall production peak, there was also higher particle concentration and bacterial
²⁶⁷ abundance in the later summer and early fall. Interestingly, while primary pro-
²⁶⁸ ductivity estimates from July-August were not that different between 2019 and
²⁶⁹ 2021 (Figure 4A), chlorophyll-a florescence, particle concentration, and bacte-
²⁷⁰ rial abundance were much higher in 2019's summer/fall (Figure 2D-F). Inorganic
²⁷¹ nutrients (*Si* and *NO₃*) were generally well stratified, with low concentrations
²⁷² in the epipelagic and increasing throughout the mesopelagic. However, both
²⁷³ nutrients did vary vertically in accordance with the 2021 February downwelling
²⁷⁴ and spring mixing period (Figure 2G-H). Additionally, in the late fall of 2021,
²⁷⁵ *Si* concentrations were slightly elevated in the mid-mesopelagic (Figure 2G).

²⁷⁶ Overall mass flux to the mesopelagic was highest during the 2021 February
²⁷⁷ downwelling (Figure 3B). Generally, export was similarly high during March,
²⁷⁸ declining in April then increasing slightly throughout the summer and early
²⁷⁹ fall. While magnitude was slightly different, this pattern was consistent with
²⁸⁰ total mass, carbon and nitrogen fluxes (Figure 3B-D). Higher mass, carbon and
²⁸¹ nitrogen flux also occurred in the 2019 late summer - early fall period.

²⁸² Rhizaria abundance and distribution

²⁸³ Across all imaged mesozooplankton (>900 μ m), Rhizaria comprised a consid-
²⁸⁴ erable fraction of the total community. Considering the total abundances of
²⁸⁵ the observational period, Rhizaria comprised on average, 42.6% of all meso-

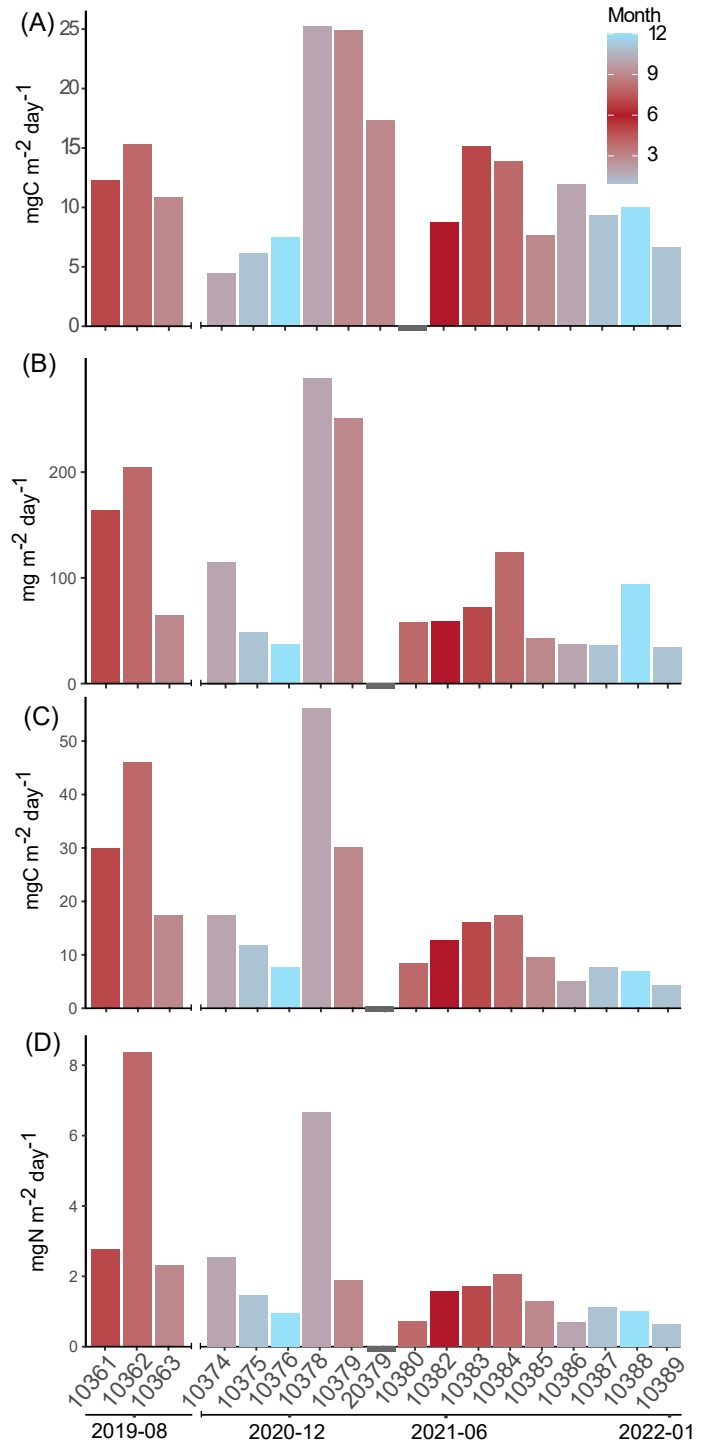


Figure 3: Primary productivity (A) and flux estimates from total mass (B), carbon (C), and nitrogen (D). Values are from monthly cruises with month displayed in corresponding colors. Absent data are shown by grey bar.

zooplankton abundance (Supplemental Figure 3). Copepods were the second
 most abundant, comprising 35.5% and all living mesozooplankton were 22%.
 The large contribution of Rhizaria to the mesozooplankton community is most
 prominent in the epipelagic, where they accounted for 47% of all mesozooplank-
 ton. In the mesopelagic rhizaria were a smaller fraction, at 38% in the upper
 layers (200-500m) and 37% in the deeper mesopelagic (500-1000m).

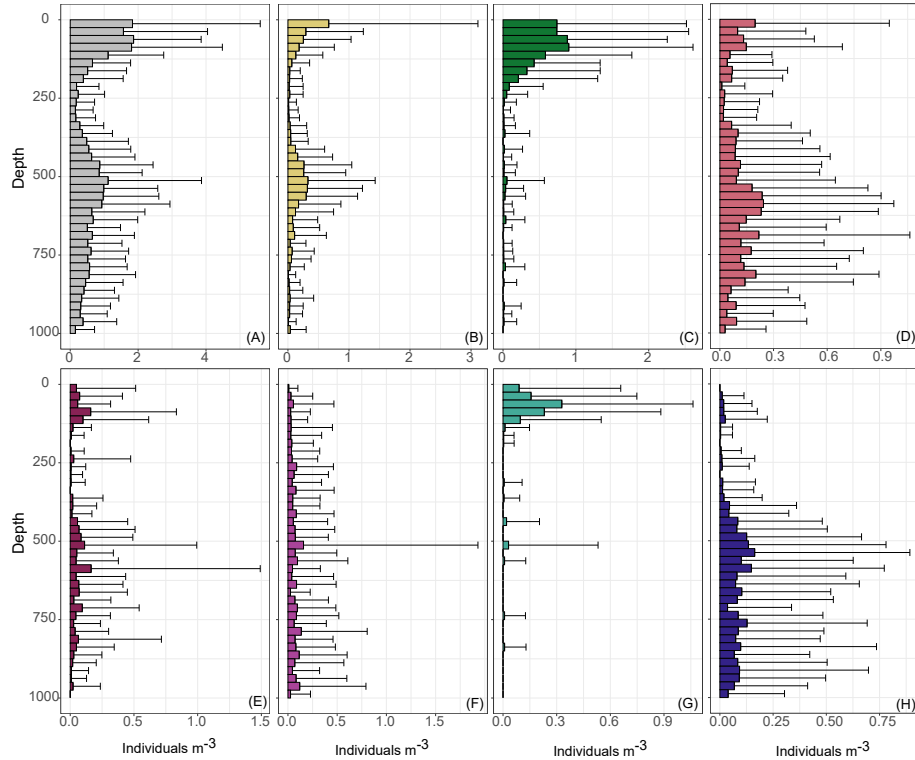


Figure 4: Average abundance of Rhizaria in 25m bins, across entire study period. Shown are total Rhizaria (A), Acantharea (B), Collodaria (C), Aulacanthidae (D), Foraminifera (E), Aulosphaeridae (F), Castanellidae (G), Coelodendridae (H).

Total average Rhizaria abundance had a bimodal distribution with respect to
 depth. Total abundance was highest just below the surface (0-100m), with

secondary, wider peak occurring in the mid mesopelagic (Figure 4A). Although, variation in depth binned abundance was large, likely due to seasonal variability but also increased from the detection-risk described in the methods. The vertical distribution pattern and abundance varied considerably across taxonomic groups. Radiolarians were some fo the most abundant taxa observed, particularly in the epipelagic (Figure 4, Figure 5B). This pattern was led by Collodaria, whose colonies were abundant in the upper epipelagic and declined into the top of the mesopelagic (Figure 4C). Acantharea displayed a bimodal distribution accounting for a large portion of the total Rhizaria pattern (Figure 4B, Figure 5). Foraminifera had a similar bimodal distribution, yet their overall average densities were much lower and spread wider throughout the mesopelagic (FIgure 4E). Phaeodarian families exhibited a wide range of vertical distribution patterns. The most abundant, Aulacanthidae, also had a bimodal pattern but the density was highest in the lower mesopelagic (Figure 4D). Aulosphaeridae had low average density and was nearly homogenously distributed throughout the water column, although slightly lower int eh epipelagic (Figure 4F). Castanelidae were the only Phaeodarian who appeared to be effectively restricted to the photic zone (Figure 4G). Alternatively, Coelodendridae primarily occurred in the lower mesopelagic (Figure 4H). A few individuals from the families Tuscaroridae and Medusettidae were also observed in the mesopelagic, yet they were much rarer (data not shown).

Between the monthly cruises, Rhizaria integrated abundance varied in the epipelagic. Highest average abundance occurred in June 2021 and was lowest

317 during the winter months (Figure 5A). The 2019 later summer - fall period
 318 also had much higher integrated abundance than similar months in 2021.
 319 While the majority of integrated abundance in the epipelagic was consistently
 320 attributable to Collodaria, Acanthrean abundance occurred sporadically and
 321 could account for a large portion of the total in some months (Figure 5B). The
 322 mesopelagic integrated abundance was much more consistent across monthly
 323 cruises, although average abundance was notably higher in 2019 (Figure 5C-F).
 324 The community composition in the mesopelagic was more diverse, mostly
 325 comprised of Phaeodarians. However, Acantharea and unidentified Rhizaria
 326 also were common members of the community (Figure 5D, 5F).

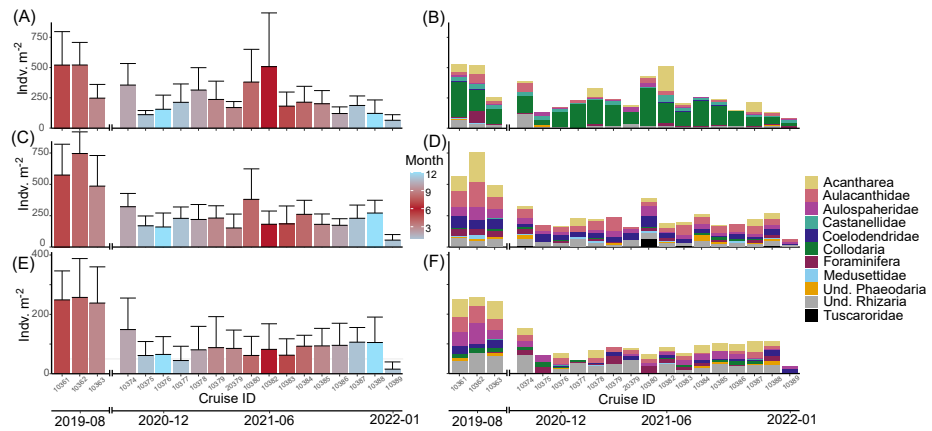


Figure 5: Seasonality of Rhizarian integrated abundance for the epipelagic (0-200m) (A-B), upper mesopelagic (200-500m) (C-D), lower mesopelagic (500-1000m) (E-F). Left panels (A,C,E) display total integrated abundance per monthly cruise colored by month. Right panels (B, D, F) display community composition of each total abundance.

327 **Environmental Drivers of Rhizarian Abundance**

328 For total Rhizarian integrated abundance the GAMs produced moderate fits
329 ($R^2_{adj} = 0.406\text{-}0.603$) (Table 1). In the epipelagic, there were several significant
330 predictor variables including inorganic nutrients (NO_3 and Si), water quality
331 parameters (Salinity, DO), primary production, and particle concentration (Ta-
332 ble 1). However, the upper and lower mesopelagic were exclusively explained
333 by particle-related variables (concentration and mass flux) (Table 1).

Table 1: Generalized Additive Model results for integrated total Rhizarian abundance in different regions of the water column.

Model	Term	edf	F	p-value
All Rhizaria Epipelagic	Salinity	2.0818	4.654	<0.001
$R^2_{adj} = 0.42$	DO	0.8272	0.945	0.0136
	Silica	3.1206	15.75	<0.001
	NO_3	2.9970	6.268	<0.001
	Primary	1.8367	2.099	<0.001
	Productivity			
	Particle	0.9282	2.566	<0.001
	Concentration			
All Rhizaria Upper	Silica	0.6847	0.431	0.073
Mesopelagic				
$R^2_{adj} = 0.406$	Avg Mass Flux	1.5426	0.923	0.045

Model	Term	edf	F	p-value
	Particle	3.2957	20.89	<0.001
	Concentration			
All Rhizaria Lower	Avg Mass Flux	1.6632	1.824	0.002
Mesopelagic				
$R^2_{adj} = 0.603$	Particle	0.7694	0.662	0.027
	Concentration			

334 GAMs for individual taxa were much less consistent in their fits (Table 2). This
 335 is likely in part due to the high number of non-observations for certain taxa.
 336 Note that due to low abundances, GAMS were not constructed for Tuscaroridae
 337 or Medusettidae. Furthermore no significant terms were found for a model with
 338 Aulosphaeridae in the epipelagic nor Foraminifera in the mesopelagic.
 339 Epipelagic Acantharea were explained by several predictor variables and had
 340 a good fit ($R^2_{adj} = 0.53$, Table 2). Most notable smooths however, were mass
 341 flux and particle concentration, which had a weak positive association (Figure
 342 6A), with July 2021 as a clear outlier where Acantharean abundances were high
 343 in the epipelagic despite lower fluxes and particle concentrations (Figure 5).
 344 Foraminifera had a good fitting GAM in the epipelagic ($R^2_{adj} = 0.445$). There
 345 were several significant explanatory variables, although the clearest pattern was
 346 observed of high temperatures associated with more Foraminifera abundance

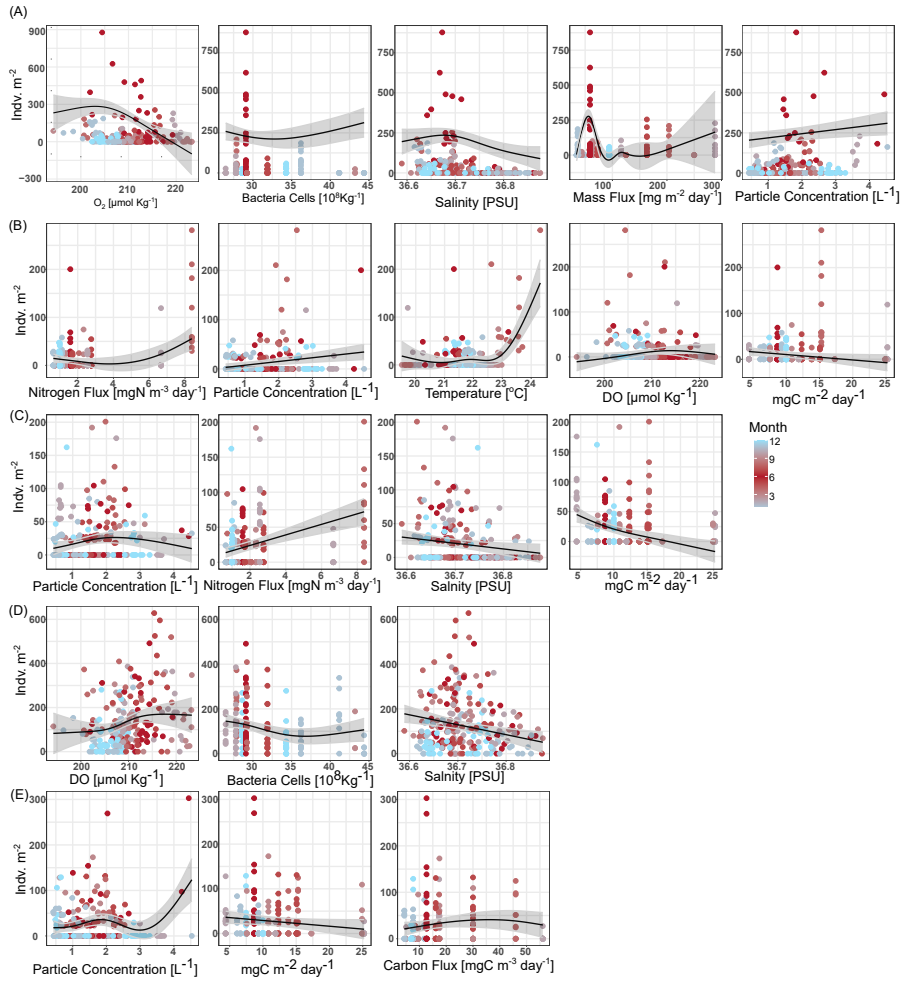


Figure 6: Partial effects of smooth terms in taxa-specific GAM models from the epipelagic (0–200m). Effects are grouped by taxa; Acantharea (A), Foraminifera (B), Aulacanthidae (C), Collodaria (D), Castanellidae (E).

347 (Table 2, Figure 6B). Epipelagic Aulacanthidae similarly had several predictor
 348 variables which were significant, including both water quality parameters and
 349 particle/flux predictors (Table 2). Interestingly, Aulacanthidae had primary
 350 production as a significant predictor, yet there was not a clear association (Fig-
 351 ure 6C). There was a fit for Collodaria in the epipelagic ($R^2_{adj} = 0.16$), although
 352 there was a logit-like relationship where higher abundances tended to occur dur-
 353 ing higher DO conditions in the surface waters (Figure 6D). Castanellidae also
 354 had similarly poor fits in the epipelagic ($R^2_{adj} = 0.124$) (Table 2, Figure 6E).

Table 2: Taxa-specific generalized additive models for different regions of the water column.

Model	Term	edf	F	p-value
Acantharea Epipelagic	Salinity	2.264	4.113	<0.001
R2adj=0.53	O2	2.579	6.712	<0.001
	Avg Mass Flux	4.810	22.81	<0.001
	Bacteria #/L	1.599	1.317	0.0117
	Particle	0.853	1.158	0.0087
	Concentration			
Acantharea Upper	Avg C Flux	1.296	0.621	0.0439
Mesopelagic				
R2adj=0.231	Avg N Flux	1.619	1.283	0.0026

Model	Term	edf	F	p-value
	Particle	0.952	3.886	<0.001
	Concentration			
Acantharea Lower	Temperature	2.076	4.155	<0.001
Mesopelagic				
R2adj=0.509	Avg N Flux	1.494	1.216	0.0113
	Primary	0.766	0.648	0.0253
	Productivity			
	Particle	2.037	10.03	<0.001
	Concentration			
Aulacanthidae Epipelagic	Salinity	0.792	0.757	0.0241
R2adj=0.251	Avg N Flux	0.869	1.324	0.0018
	Primary	2.312	7.704	<0.001
	Productivity			
	Particle	2.008	2.200	0.0017
	Concentration			
Aulacanthidae Upper	Particle	2.832	9.802	<0.001
Mesopelagic	Concentration			
R2adj = 0.158				

Model	Term	edf	F	p-value
Aulacanthidae Lower	Avg Mass Flux	1.622	1.991	0.002
Mesopelagic				
R2adj=0.298	Particle	2.123	6.706	<0.001
	Concentration			
Aulosphaeridae Upper	Particle	2.653	13.06	<0.001
Mesopelagic	Concentration			
R2adj=0.2				
Aulosphaeridae Lower	Particle	0.972	6.248	<0.001
Mesopelagic	Concentration			
R2adj=.147				
Castanellidae Epipelagic	Avg C Flux	1.462	0.816	0.0421
R2adj = 0.124	Primary	0.771	0.665	0.0247
	Productivity			
	Particle	3.956	4.623	<0.001
	Concentration			
Coelodendridae Upper	Avg N Flux	0.822	0.919	0.0183
Mesopelagic				

Model	Term	edf	F	p-value
R2adj=.113	Particle	0.970	6.208	<0.001
	Concentration			
Coelodendridae Lower	Particle	1.773	4.873	<0.001
Mesopelagic	Concentration			
R2adj=.133				
Collodaria Epipelagic	Salinity	0.925	2.267	<0.001
R2adj=0.16	O2	2.015	2.217	0.002
	Bacteria #/L	1.843	2.100	0.002
Foraminifera Epipelagic	Temperature	4.414	8.789	<0.001
R2adj=0.445	O2	1.603	1.287	0.0111
	Avg N Flux	2.512	3.396	<0.001
	Primary	0.824	0.920	0.0153
	Productivity			
	Particle	0.919	2.257	<0.001
	Concentration			

³⁵⁵ In the upper mesopelagic (200-500m), abundances were generally low (Figure

³⁵⁶ 4) so GAMs were only constructed for Acantharea, Aulacanthidae, Aulosphaeri-

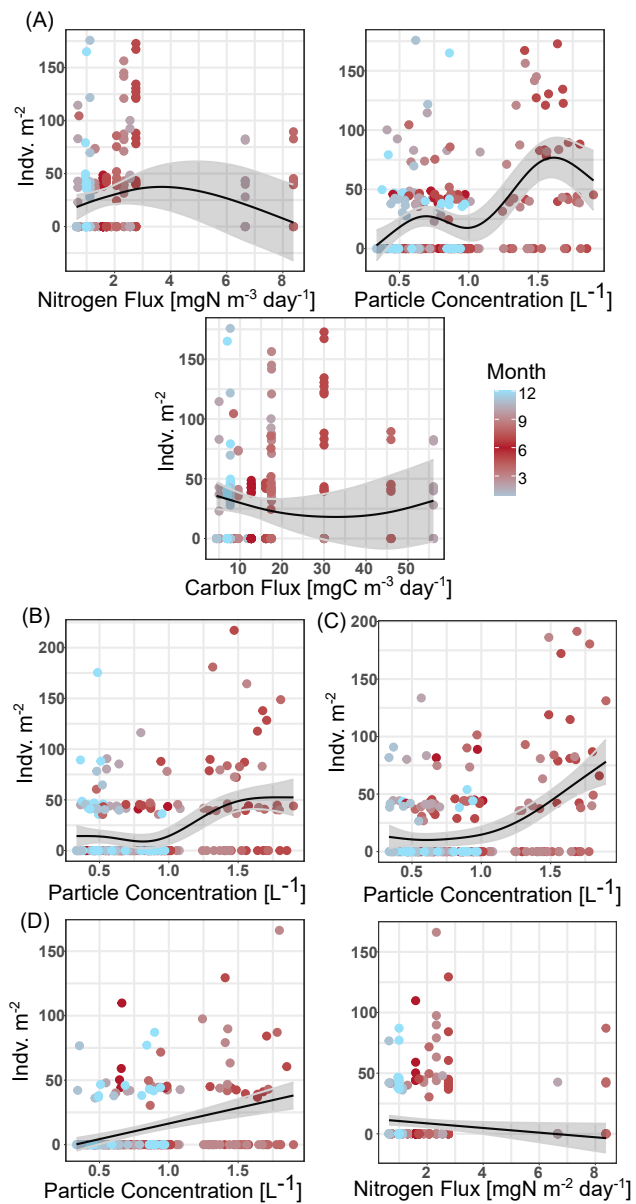


Figure 7: Partial effects of smooth terms in taxa-specific GAM models from the upper mesopelagic (200-500m). Effects are grouped by taxa; Acantharea (A), Aulacanthidae (B), Aulosphaeridae (C), Coelodendridae (D).

dae, and Coelodendridae (Table 2). All these models had generally poor fits ($R^2_{adj} < 0.25$). Yet, for all upper mesopelagic models, particle concentration was a significant explanatory variable (Table 2, Figure 7). Carbon flux was significant for Acantharea and nitrogen flux was significant for both Acantharea and Coelodendridae (Table 2, Figure 7A,D). The lower mesopelagic also had generally poor GAM fits for taxa specific models ($R^2_{adj} < 0.3$), with the exception of Acantharea ($R^2_{adj} = 0.509$). Acantharea in the lower mesopelagic was most clearly positively associated with particle concentration and nitrogen flux, as well as temperature to a slight degree (Figure 8A). For all Phaeodarians with a significant model, particle concentration was a main predictor variable (Table 2, Figure 8B-D). Aulacanthidae had the best fitting model of the Phaeodarians ($R^2_{adj} = 0.298$), which also included mass flux as a statistically significant smooth (Figure 8B).

370 Discussion

371 Overall Rhizarian abundance and patterns

372 In the epipelagic Rhizaria exhibited a notable seasonal pattern. Rhizarian abundances were higher in the summer months and lower during the winter. During 373 a prior time period, Blanco-Bercial et al. (2022) noted that there is considerable 374 seasonality in the community composition of all protists. Despite the seasonality 375 of total Rhizarian abundance, community composition was relatively consistent, 376 with Collodaria representing the bulk of the community. It should be noted that 377

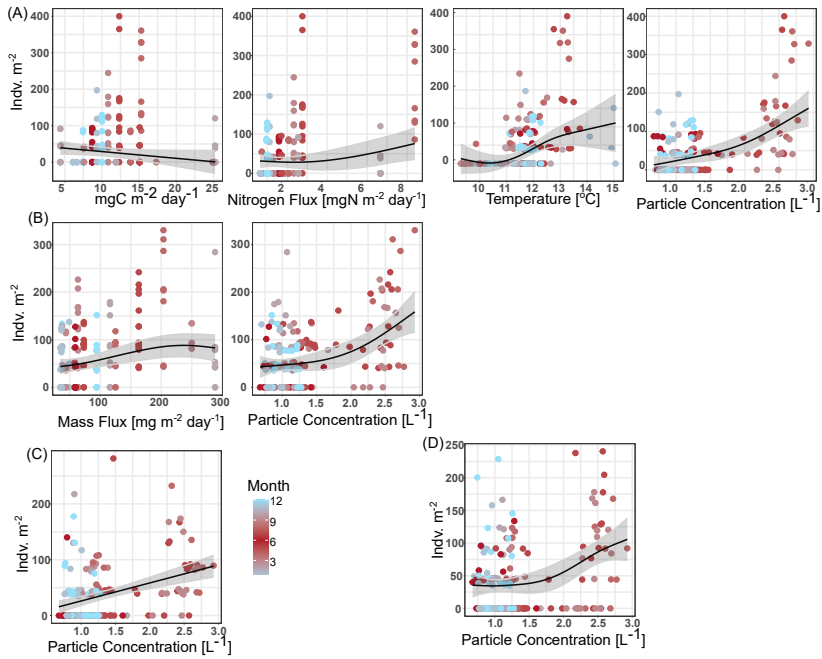


Figure 8: Partial effects of smooth terms in taxa-specific GAM models from the lower mesopelagic (500-1000m). Effects are grouped by taxa; Acantharea (A), Aulacanthidae (B), Aulosphaeridae (C), Coelodendriidae (D).

³⁷⁸ the overall taxonomic resolution of the UVP5 is fairly low, so there may be a
³⁷⁹ switching of species within the broad groups identified in this study which were
³⁸⁰ not captured. Throughout the mesopelagic, month-to-month variation in 2021
³⁸¹ was relatively low. Again this is consistent with observations from metabarcod-
³⁸² ing of the whole protist community in the same study region (Blanco-Bercial
³⁸³ et al., 2022). This finding is not surprising as the overall seasonal variation in
³⁸⁴ environmental conditions in this region were low.

³⁸⁵ Overall Rhizaria were the most commonly identified group of mesozooplankton
³⁸⁶ throughout the study period. We do note that the UVP5 commonly captures
³⁸⁷ Trichodesmium colonies, yet these were excluded in this comparison as they
³⁸⁸ are strictly autotrophs. It should be noted that previous work has suggested
³⁸⁹ that avoidance behavior with the UVP is possible, at times likely, for visual and
³⁹⁰ highly mobile zooplankton (Barth and Stone, 2022). Thus, the percent contribu-
³⁹¹ tion reported here (42.7%) of Rhizaria to the total mesozooplankton community
³⁹² may be inflated due to under sampling of organisms such as Euphausiids and
³⁹³ Chaetognaths which has quick escape responses. Regardless, it is worth noting
³⁹⁴ that in the same region, with data collected in 2012 and 2013 using similar cal-
³⁹⁵ culation methods, Biard et al. (2016) estimated Rhizaria only contribute 15%
³⁹⁶ of the total mesozooplankton community in the upper 500m. Likely, Rhizaria
³⁹⁷ display considerable interannual variability. In the present study, we noticed
³⁹⁸ considerably higher Rhizarian abundance throughout the water column in 2019
³⁹⁹ compared to 2021. While this may have been driven by increased mass flux
⁴⁰⁰ (Figure 3), more information is needed to truly understand the magnitude by

⁴⁰¹ which Rhizaria can vary interannually.

⁴⁰² **Vertical Structure and Trophic Roles**

⁴⁰³ In this study we present a clear pattern of vertical zonation between different
⁴⁰⁴ Rhizaria groups. Largely, the taxonomic composition and vertical positioning
⁴⁰⁵ were similar to Rhizaria zonation in the California Current Ecosystem (Biard
⁴⁰⁶ and Ohman, 2020). It should be noted however, that the secondary abun-
⁴⁰⁷ dance peak reported in the present study is lower. This is likely due to the
⁴⁰⁸ more oligotrophic nature of the study region, where the euphotic zone penetrates
⁴⁰⁹ deeper into the water column. Most prevalent in the epipelagic were Collo-
⁴¹⁰ daria. These mixotrophic Radiolarians have long been reported to contribute
⁴¹¹ to primary productivity in the euphotic zone (Dennett et al., 2002; Michaels et
⁴¹² al., 1995). Collodaria are thought to be particularly successful globally in olig-
⁴¹³ otrophic regions due to their photosymbiotic relationships (Biard et al., 2017,
⁴¹⁴ 2016). We observed the highest abundance of Collodaria during June 2021,
⁴¹⁵ supporting the notion they can thrive during the typically low-nutrient condi-
⁴¹⁶ tions of summer stratification. However, Collodaria also increased during the
⁴¹⁷ spring mixing period, suggesting that they can thrive during conditions which
⁴¹⁸ may typically be thought to favor autotrophs. Furthermore, while Collodaria
⁴¹⁹ were primarily absent from below 250m, there were a few instances of deeper
⁴²⁰ colonies being observed. Global investigations of polycistine flux, suggest that
⁴²¹ deep-Collodaria in Oligotrophic regions may be a consequence of isothermal sub-
⁴²² mersion (Boltovskoy, 2017). Another effectively exclusively epipelagic Rhizaria

423 was the Phaeodarian family of Castanellidae. All Phaeodarians are thought to
424 be fully heterotrophic (Nakamura and Suzuki, 2015), nonetheless a number of
425 studies, including this one, report Castanellidae to be typically found in the
426 lower epipelagic (Biard et al., 2018; Biard and Ohman, 2020; Zasko and Ru-
427 sanov, 2005). It should be considered that perhaps Castanellidae specializes
428 in feeding sinking particles directly at the base of the epipelagic. Given it's
429 smaller size (Nakamura and Suzuki, 2015), Castanellidae does not need a large
430 diameter to efficiently flux feed at the typically particle rich region of the lower
431 epipelagic. Both Castanellidae and Collodaria had poor fitting GAMs. This is
432 somewhat of a surprise for Collodaria who had large abundance. However, given
433 the consistency of their abundance, it may be that this study did not capture a
434 wide enough range of conditions for describing Collodaria's preferred niche.

435 The mesopelagic generally was home to known heterotrophic organisms,
436 particularly for those which were constrained to exclusively occupy deeper
437 waters. This is consistent with Blanco-Bercial et al. (2022)'s observation of
438 an auto-/mixotroph to heterotroph gradient in the protist community. The
439 upper mesopelagic interestingly had relatively low total abundance. This
440 low-abundance region likely reflects the dynamics of productivity and export
441 throughout the water column. While productivity and thus sinking particles for
442 flux feeders are high in the euphotic zone, much of this is attenuated throughout
443 the epipelagic. So, while the base of the epipelagic may provide a rich feeding
444 environment for Castanellidae, smaller protists, or heterotrophic bacteria
445 (Figure 2F), the region from 200-500m might be otherwise food poor. Perhaps

446 it is more advantageous for Rhizaria to situate deeper, in darker regions of the
447 twilight zone. Also it should be noted that Phaeodarians utilize silica to build
448 their opaline tests, and silica concentrations started to increase around 500m
449 (Figure 2G). Although *Si* was not a significant smooth for any taxa-specific
450 model, this lack of association might be due to the overall lack of variation of *Si*
451 between integrated abundance of each cast. Aulosphaeridae was only found to
452 have significant relationships, although weak fits, to particle concentration in
453 the mesopelagic. In our study, while consistently observed, overall abundances
454 of Aulosphaeridae were very low. In the Pacific Ocean, on California's Coast,
455 much higher abundances of Aulosphaeridae have been reported (Biard and
456 Ohman, 2020; Zasko and Rusanov, 2005) and they have massive potential to
457 impact silica export (Biard et al., 2018). Coelodendridae were also seemingly
458 restricted to the deeper section of the mesopelagic. This is interesting given
459 that in the California Current, (Biard and Ohman, 2020) found a bimodal
460 distribution in Coelodendridae. There are several morphotypes corresponding
461 to different taxa of Coelodendridae (Biard and Ohman, 2020; Nakamura and
462 Suzuki, 2015). So it may be that only a few types of Coelodendridae were
463 observed in this study, while the epipelagic variety was not. Alternatively, the
464 lower epipelagic of the California Current may provide adequate habitat for
465 Coelodendridae, which is not available in the oligotrophic Sargasso Sea.

466 A number of taxa were found to have a bimodal distribution, with considerable
467 populations in both the epipelagic and mesopelagic. Aulacanthidae had a bi-
468 modal distribution, although abundances were highest in the lower mesopelagic.

⁴⁶⁹ Foraminifera also had a bimodal distribution. Some lineages of Foraminifera
⁴⁷⁰ are known to host photosymbionts (Biard, 2022a; Kimoto, 2015), however they
⁴⁷¹ are also efficient predators commonly seen throughout the mesopelagic (Caron
⁴⁷² and Be, 1984; Gaskell et al., 2019). Thus it is not surprising to find their pres-
⁴⁷³ ence in both locations of the water column. Foraminifera are also known to
⁴⁷⁴ vary their vertical distribution across their life cycle in phase with lunar cycles
⁴⁷⁵ (Biard, 2022a; Bijma et al., 1990; Gaskell et al., 2019; Kimoto, 2015). However,
⁴⁷⁶ the sampling scheme of the BATS program does not capture this frequency and
⁴⁷⁷ was not investigated in the present study.

⁴⁷⁸ Acantharea also had a bimodal distribution, with much larger abundances than
⁴⁷⁹ Aulacanthidae or Foraminifera. Most prior studies of Acantharea vertical dis-
⁴⁸⁰ tribtion found them concentrated in near surface layers of the water column
⁴⁸¹ Zasko and Rusanov (2005). This would support the paradigm that large Acan-
⁴⁸² tharean abundances may be supported by their mixotrophic abilities (Michaels
⁴⁸³ et al., 1995; Suzuki and Not, 2015). While the UVP5 images cannot distinguish
⁴⁸⁴ between mixotrophic and heterotrophic Acantharea, the GAMs constructed for
⁴⁸⁵ Acantharean abundance found positive associations with particle concentration
⁴⁸⁶ and mass flux, suggesting a higher reliance on heterotrophy. Recently Mars Bris-
⁴⁸⁷ bin et al. (2020) described apparent predator behavior amongst near-surface
⁴⁸⁸ Acantharea. Thus it is likely that epipelagic Acantharea may commonly be
⁴⁸⁹ heterotrophic. Yet, it should be noted in the Sargasso Sea, both heterotrophic
⁴⁹⁰ and symbiotic lineages of Acantharea have been reported (Blanco-Bercial et al.,
⁴⁹¹ 2022). Additionally, Michaels (1988) noted that the majority of Acantharea (by

⁴⁹² abundance) were smaller than $160\mu m$. While that estimate may be inflated due
⁴⁹³ to inability to capture larger cells, small Acantharea were not captured in the
⁴⁹⁴ present study. Thus, trophic strategy may shift based on sizes of Acantharea.

⁴⁹⁵ Decelle et al. (2013) proposed a hypothetical life cycle for cyst-bearing
⁴⁹⁶ (strictly heterotrophic) Acantharea. This hypothesized life cycle suggests
⁴⁹⁷ that epipelagic Acantharea are adult populations, which form cysts that sink
⁴⁹⁸ into the mesopelagic, then reproduce and raise. Furthermore, given that
⁴⁹⁹ horizontal transfer of symbionts between generations of Acantharea is unlikely,
⁵⁰⁰ the newly spawned mesopelagic Acantharea are not necessarily required to
⁵⁰¹ rapidly return to the photic zone. This hypothesis predicts that Acanthareans
⁵⁰² in the mesopelagic would be smaller (Decelle et al., 2013). Mars Brisbin
⁵⁰³ et al. (2020) provided some support for this hypothesis, with a significant
⁵⁰⁴ decrease in Acantharea sizes with depth. Although, the authors also observed
⁵⁰⁵ low abundances in the mesopelagic and noted that the smaller sizes may be
⁵⁰⁶ due to less food availability (Mars Brisbin et al., 2020). Since food is more
⁵⁰⁷ scarce in the mesopelagic there is less nutritional quality, yet flux feeders
⁵⁰⁸ would likely grow larger to increase their feeding range (Biard and Ohman,
⁵⁰⁹ 2020). In the data collecting in this study, Acanthareans in the mesopelagic
⁵¹⁰ were significantly smaller than the epipelagic, despite the other bimodal taxa
⁵¹¹ (Foraminifera and Aulacanthidae) being significantly larger with depth (Figure
⁵¹² 9, Wilcoxon rank sum test p-value < 0.001). This provides added support for
⁵¹³ the hypothesis that cyst-forming Acantharea may utilize different sections of
⁵¹⁴ the water column throughout their life cycle. However to further investigate

515 this, more work is needed with higher temporal and taxonomic resolution.

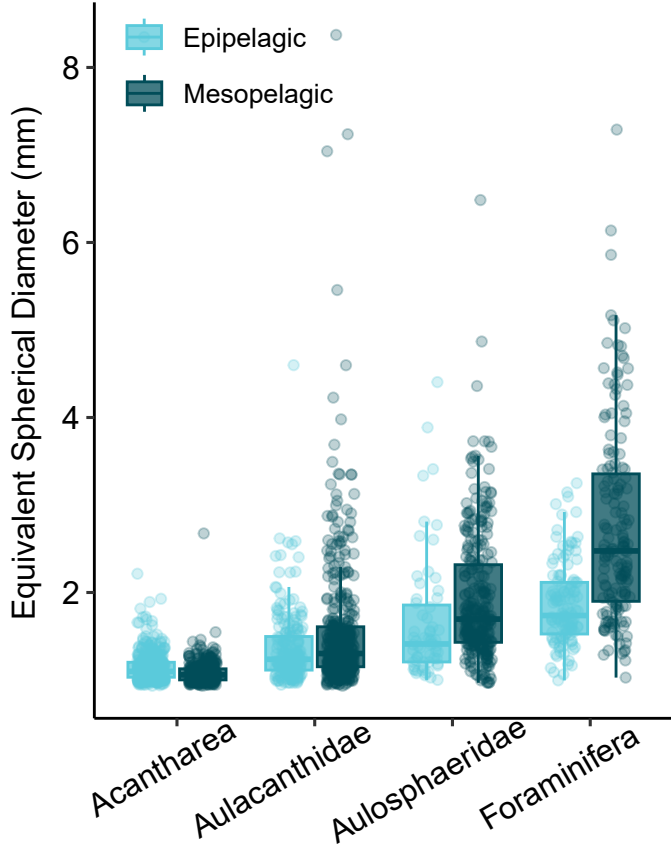


Figure 9: Comparison of average sizes (ESD) amongst Rhizarian taxa which occurred throughout the water column.

516 **Conclusions and Considerations**

517 This study provides a detailed look at Rhizarian abundance over time through-
518 out the water column in a major oligotrophic gyre. We show that their abun-
519 dances are generally related to particle concentration and flux, although lack
520 of environmental variability may have reduced the fit of our GAMs. Consid-
521 ering the potential role of Rhizaria in the biological carbon pump, they may

522 have a somewhat mixed role. In the shallower regions, where smaller Rhizaria
523 are abundant, they may be an attenuating force on sinking particles (Stukel
524 et al., 2019). It should be noted that in our study, we focused on the “small”
525 particle concentration field ($<450\mu m$), and these particles are generally slower
526 sinking than large particles. However, once consumed and repackaged by larger
527 Rhizaria, they can sink quicker and contribute more to overall flux (Michaels,
528 1988). Thus, Rhizaria may act as a ballasting mechanism. However, this is
529 largely speculation, to truly test this, more work is needed measuring Rhizarian
530 flux.

531 The vertical partitioning documented in this study do support the hypothesis
532 that mixotrophic rhizaria will occupy shallower waters while deeper waters are
533 dominated by heterotrophy. However the degree to which mixotrophic Rhizaria
534 in the euphotic zone rely on heterotrophy versus symbiosis is uncertain. Col-
535 lodaria were recorded as consistent and dominant members of the near surface
536 region. These organisms have the potential to contribute considerably to the
537 otherwise low productivity of oligotrophic regions. However, their role in food
538 webs is not well understood. While this study represents a step-forward in our
539 understanding of Rhizarian ecology, there are several known aspects of Rhizar-
540 ian and protist ecology which are not captured in this study. Continued research
541 on Rhizaria is much needed to better understand their ecology. Particularly ex-
542 tended descriptive work to capture interannual patterns. Also work defining
543 biotic interactions, feeding rates, productivity, and life history are all rich fields
544 of interest in Rhizaria.

545 **References:**

- 546 Anderson, O.R., 2014. Living Together in the Plankton: A Survey of Marine
547 Protist Symbioses. *Acta Protozoologica* 53, 29–38. <https://doi.org/10.4467/16890027AP.13.0019.1116>
- 548 549 Anderson, O.R., Bé, A.W.H., 1976. A CYTOCHEMICAL FINE STRUCTURE
550 STUDY OF PHAGOTROPHY IN A PLANKTONIC FORAMINIFER,
551 *HASTIGERINA PELAGICA* (d'ORBIGNY). *The Biological Bulletin* 151,
552 437–449. <https://doi.org/10.2307/1540498>
- 553 554 Aurahs, R., Grimm, G.W., Hemleben, V., Hemleben, C., Kucera, M., 2009. Ge-
ographical distribution of cryptic genetic types in the planktonic foraminifer
555 *Globigerinoides ruber*. *Molecular Ecology* 18, 1692–1706. <https://doi.org/10.1111/j.1365-294X.2009.04136.x>
- 556 557 Barth, A., Stone, J., in review. Understanding the picture: The promises and
challenges of in-situ imagery data in the study of plankton ecology.
- 558 559 Barth, A., Stone, J., 2022. Comparison of an in situ imaging device and net-
560 based method to study mesozooplankton communities in an oligotrophic
561 system. *Frontiers in Marine Science* 9.
- 562 Benfield, M.C., Davis, C.S., Wiebe, P.H., Gallager, S.M., Gregory Lough, R.,
563 Copley, N.J., 1996. Video Plankton Recorder estimates of copepod, ptero-
564 pod and larvacean distributions from a stratified region of Georges Bank
565 with comparative measurements from a MOCNESS sampler. *Deep Sea
566 Research Part II: Topical Studies in Oceanography* 43, 1925–1945. [https://doi.org/10.1016/S0967-0645\(96\)00044-6](https://doi.org/10.1016/S0967-0645(96)00044-6)

- 568 Biard, T., 2022a. Rhizaria. Encyclopeida of Life Sciences, pp. 1–11. <https://doi.org/10.1002/9780470015902.a0029469>
- 569
570 Biard, T., 2022b. Diversity and ecology of Radiolaria in modern oceans. Envi-
ronmental Microbiology 24, 2179–2200. <https://doi.org/10.1111/1462-2920.16004>
- 571
572 Biard, T., Bigeard, E., Audic, S., Poulain, J., Gutierrez-Rodriguez, A., Pesant,
S., Stemmann, L., Not, F., 2017. Biogeography and diversity of Collodaria
(Radiolaria) in the global ocean. The ISME Journal 11, 1331–1344. <https://doi.org/10.1038/ismej.2017.12>
- 573
574 Biard, T., Krause, J.W., Stukel, M.R., Ohman, M.D., 2018. The Significance
of Giant Phaeodarians (Rhizaria) to Biogenic Silica Export in the California
575 Current Ecosystem. Global Biogeochemical Cycles 32, 987–1004. <https://doi.org/10.1029/2018GB005877>
- 576
577 Biard, T., Ohman, M.D., 2020. Vertical niche definition of test-bearing protists
(Rhizaria) into the twilight zone revealed by in situ imaging. Limnology and
578 Oceanography 65, 2583–2602. <https://doi.org/10.1002/lno.11472>
- 579
580 Biard, T., Pillet, L., Decelle, J., Poirier, C., Suzuki, N., Not, F., 2015. To-
wards an integrative morpho-molecular classification of the collodaria (poly-
581 cystinea, radiolaria). Protist 166, 374–388. <https://doi.org/10.1016/j.protis.2015.05.002>
- 582
583 Biard, T., Stemmann, L., Picheral, M., Mayot, N., Vandromme, P., Hauss, H.,
Gorsky, G., Guidi, L., Kiko, R., Not, F., 2016. In situ imaging reveals
584 the biomass of giant protists in the global ocean. Nature 532, 504–507.

- 591 <https://doi.org/10.1038/nature17652>
- 592 Bijma, J., Erez, J., Hemleben, C., 1990. Lunar and semi-lunar reproductive
593 cycles in some spinose planktonic foraminifers. Journal of Foraminiferal
594 Research 20, 117–127.
- 595 Blanco-Bercial, L., Parsons, R., Bolaños, L.M., Johnson, R., Giovannoni, S.J.,
596 Curry, R., 2022. The protist community traces seasonality and mesoscale
597 hydrographic features in the oligotrophic sargasso sea. Frontiers in Marine
598 Science 9.
- 599 Boltovskoy, D., 2017. Vertical distribution patterns of radiolaria polycystina
600 (protista) in the world ocean: Living ranges, isothermal submersion and
601 settling shells. Journal of Plankton Research 39, 330–349. <https://doi.org/10.1093/plankt/fbx003>
- 602
- 603 Boltovskoy, D., Alder, V.A., Abelmann, A., 1993. Annual flux of radiolaria and
604 other shelled plankters in the eastern equatorial atlantic at 853 m: seasonal
605 variations and polycystine species-specific responses. Deep Sea Research
606 Part I: Oceanographic Research Papers 40, 1863–1895. [https://doi.org/10.1016/0967-0637\(93\)90036-3](https://doi.org/10.1016/0967-0637(93)90036-3)
- 607
- 608 Caron, D.A., 2016. The rise of rhizaria | nature. Nature 532, 444–445.
- 609 Caron, D.A., Be, A.W.H., 1984. PREDICTED AND OBSERVED FEEDING
610 RATES OF THE SPINOSE PLANKTONIC FORAMINIFER. BULLETIN
611 OF MARINE SCIENCE 35.
- 612 Caron, D.A., Michaels, A.F., Swanberg, N.R., Howse, F.A., 1995. Primary pro-
613 ductivity by symbiont-bearing planktonic sarcodines (acantharia, radiolaria,

- 614 foraminifera) in surface waters near bermuda. Journal of Plankton Research
615 17, 103–129. <https://doi.org/10.1093/plankt/17.1.103>
- 616 Cavalier-Smith, T., Chao, E.E., Lewis, R., 2018. Multigene phylogeny and cell
617 evolution of chromist infrakingdom Rhizaria: contrasting cell organisation of
618 sister phyla Cercozoa and Retaria. Protoplasma 255, 1517–1574. <https://doi.org/10.1007/s00709-018-1241-1>
- 620 Cohen, N.R., Krinos, A.I., Kell, R.M., Chmiel, R.J., Moran, D.M., McIlvin,
621 M.R., Lopez, P.Z., Barth, A., Stone, J., Alanis, B.A., Chan, E.W., Breier,
622 J.A., Jakuba, M.V., Johnson, R., Alexander, H., Saito, M.A., 2023. Mi-
623 croeukaryote metabolism across the western North Atlantic Ocean revealed
624 through autonomous underwater profiling. <https://doi.org/10.1101/2023.11.20.567900>
- 626 Decelle, J., Colin, S., Foster, R.A., 2015. Photosymbiosis in Marine Planktonic
627 Protists, in: Ohtsuka, S., Suzuki, T., Horiguchi, T., Suzuki, N., Not, F.
628 (Eds.), Springer Japan, Tokyo, pp. 465–500. https://doi.org/10.1007/978-4-431-55130-0_19
- 630 Decelle, J., Martin, P., Paborstava, K., Pond, D.W., Tarling, G., Mahé, F., De
631 Vargas, C., Lampitt, R., Not, F., 2013. Diversity, Ecology and Biogeochem-
632 istry of Cyst-Forming Acantharia (Radiolaria) in the Oceans. PLoS ONE 8,
633 e53598. <https://doi.org/10.1371/journal.pone.0053598>
- 634 Decelle, J., Siano, R., Probert, I., Poirier, C., Not, F., 2012. Multiple microalgal
635 partners in symbiosis with the acantharian Acanthochiasma sp. (Radiolaria).
636 Symbiosis 58, 233–244. <https://doi.org/10.1007/s13199-012-0195-x>

- 637 Dennett, M.R., Caron, D.A., Michaels, A.F., Gallager, S.M., Davis, C.S., 2002.
- 638 Video plankton recorder reveals high abundances of colonial radiolaria in
- 639 surface waters of the central north pacific. Journal of Plankton Research 24,
- 640 797–805. <https://doi.org/10.1093/plankt/24.8.797>
- 641 Drago, L., Panaïotis, T., Irisson, J.-O., Babin, M., Biard, T., Carlotti, F.,
- 642 Coppola, L., Guidi, L., Hauss, H., Karp-Boss, L., Lombard, F., McDon-
- 643 nell, A.M.P., Picheral, M., Rogge, A., Waite, A.M., Stemmann, L., Kiko,
- 644 R., 2022. Global Distribution of Zooplankton Biomass Estimated by In
- 645 Situ Imaging and Machine Learning. Frontiers in Marine Science 9. <https://doi.org/10.3389/fmars.2022.894372>
- 647 Gaskell, D.E., Ohman, M.D., Hull, P.M., 2019. Zooglider-based measurements
- 648 of planktonic foraminifera in the californian current system. Journal of
- 649 Foraminiferal Research 49, 390–404. <https://doi.org/10.2113/gsjfr.49.4.390>
- 650 Guidi, L., Chaffron, S., Bittner, L., Eveillard, D., Larhlimi, A., Roux, S.,
- 651 Darzi, Y., Audic, S., Berline, L., Brum, J.R., Coelho, L.P., Espinoza, J.C.I.,
- 652 Malviya, S., Sunagawa, S., Dimier, C., Kandels-Lewis, S., Picheral, M.,
- 653 Poulain, J., Searson, S., Stemmann, L., Not, F., Hingamp, P., Speich, S.,
- 654 Follows, M., Karp-Boss, L., Boss, E., Ogata, H., Pesant, S., Weissenbach, J.,
- 655 Wincker, P., Acinas, S.G., Bork, P., Vargas, C. de, Iudicone, D., Sullivan,
- 656 M.B., Raes, J., Karsenti, E., Bowler, C., Gorsky, G., 2016. Plankton net-
- 657 works driving carbon export in the oligotrophic ocean. Nature 532, 465–470.
- 658 <https://doi.org/10.1038/nature16942>
- 659 Gutierrez-Rodriguez, A., Stukel, M.R., Lopes dos Santos, A., Biard, T., Scharek,

- 660 R., Vaulot, D., Landry, M.R., Not, F., 2019. High contribution of Rhizaria
661 (Radiolaria) to vertical export in the California Current Ecosystem revealed
662 by DNA metabarcoding. *The ISME Journal* 13, 964–976. <https://doi.org/10.1038/s41396-018-0322-7>
- 663
- 664 Gutiérrez-Rodríguez, A., Lopes dos Santos, A., Safi, K., Probert, I., Not, F.,
665 Fernández, D., Gourvil, P., Bilewitch, J., Hulston, D., Pinkerton, M., Nod-
666 der, S.D., 2022. Planktonic protist diversity across contrasting subtropical
667 and subantarctic waters of the southwest pacific. *Progress in Oceanography*
668 206, 102809. <https://doi.org/10.1016/j.pocean.2022.102809>
- 669
- 670 Haekel, E., 1887. Report on the radiolaria collected by h.m.s. Challenger during
the years 1873-1876, plates, by ernst haekel.
- 671
- 672 Hull, P.M., Osborn, K.J., Norris, R.D., Robison, B.H., 2011. Seasonality and
depth distribution of a mesopelagic foraminifer, *Hastigerinella digitata*, in
673 Monterey Bay, California. *Limnology and Oceanography* 56, 562–576. <https://doi.org/10.4319/lo.2011.56.2.0562>
- 674
- 675 Ikenoue, T., Kimoto, K., Okazaki, Y., Sato, M., Honda, M.C., Takahashi, K.,
676 Harada, N., Fujiki, T., 2019. Phaeodaria: An Important Carrier of Particu-
677 late Organic Carbon in the Mesopelagic Twilight Zone of the North Pacific
678 Ocean. *Global Biogeochemical Cycles* 33, 1146–1160. <https://doi.org/10.1029/2019GB006258>
- 679
- 680 Kimoto, K., 2015. Planktic foraminifera. pp. 129–178. https://doi.org/10.1007/978-4-431-55130-0_7
- 681
- 682 Lampitt, R.S., Salter, I., Johns, D., 2009. Radiolaria: Major exporters of or-

683 ganic carbon to the deep ocean. Global Biogeochemical Cycles 23. <https://doi.org/10.1029/2008GB003221>

684

685 Lee, J.J., 2006. [Algal symbiosis in larger foraminifera](#). Symbiosis 42, 63–75.

686 Llopis Monferrer, N., Biard, T., Sandin, M.M., Lombard, F., Picheral, M., Elin-

687 eau, A., Guidi, L., Leynaert, A., Tréguer, P.J., Not, F., 2022. [Siliceous](#)

688 [rhizaria abundances and diversity in the mediterranean sea assessed by com-](#)

689 [bined imaging and metabarcoding approaches](#). Frontiers in Marine Science

690 9.

691 Llopis Monferrer, N., Leynaert, A., Tréguer, P., Gutiérrez-Rodríguez, A.,

692 Moriceau, B., Gallinari, M., Latasa, M., L'Helguen, S., Maguer, J.-F., Safi,

693 K., Pinkerton, M.H., Not, F., 2021. Role of small Rhizaria and diatoms

694 in the pelagic silica production of the Southern Ocean. Limnology and

695 Oceanography 66, 2187–2202. <https://doi.org/10.1002/lno.11743>

696 Lomas, M.W., Bates, N.R., Johnson, R.J., Knap, A.H., Steinberg, D.K., Carl-

697 son, C.A., 2013. Two decades and counting: 24-years of sustained open ocean

698 biogeochemical measurements in the Sargasso Sea. Deep Sea Research Part

699 II: Topical Studies in Oceanography 93, 16–32. <https://doi.org/10.1016/j.dsro.2013.01.008>

700

701 Lombard, F., Boss, E., Waite, A.M., Vogt, M., Uitz, J., Stemmann, L., Sosik,

702 H.M., Schulz, J., Romagnan, J.-B., Picheral, M., Pearlman, J., Ohman,

703 M.D., Niehoff, B., Möller, K.O., Miloslavich, P., Lara-Lpez, A., Kudela, R.,

704 Lopes, R.M., Kiko, R., Karp-Boss, L., Jaffe, J.S., Iversen, M.H., Irisson,

705 J.-O., Fennel, K., Hauss, H., Guidi, L., Gorsky, G., Giering, S.L.C., Gaube,

706 P., Gallager, S., Dubelaar, G., Cowen, R.K., Carlotti, F., Briseño-Avena,
707 C., Berline, L., Benoit-Bird, K., Bax, N., Batten, S., Ayata, S.D., Artigas,
708 L.F., Appeltans, W., 2019. [Globally consistent quantitative observations of](#)
709 [planktonic ecosystems](#). Frontiers in Marine Science 6.

710 Marra, G., Wood, S.N., 2011. Practical variable selection for generalized ad-
711 ditive models. Computational Statistics & Data Analysis 55, 2372–2387.
712 <https://doi.org/10.1016/j.csda.2011.02.004>

713 Mars Brisbin, M., Brunner, O.D., Grossmann, M.M., Mitarai, S., 2020. Paired
714 high-throughput, in situ imaging and high-throughput sequencing illuminate
715 acantharian abundance and vertical distribution. Limnology and Oceanog-
716 raphy 65, 2953–2965. <https://doi.org/10.1002/lno.11567>

717 McGillicuddy, D.J., Robinson, A.R., Siegel, D.A., Jannasch, H.W., Johnson,
718 R., Dickey, T.D., McNeil, J., Michaels, A.F., Knap, A.H., 1998. Influence
719 of mesoscale eddies on new production in the Sargasso Sea. Nature 394,
720 263–266. <https://doi.org/10.1038/28367>

721 Michaels, A.F., 1988. Vertical distribution and abundance of Acantharia and
722 their symbionts. Marine Biology 97, 559–569. <https://doi.org/10.1007/BF00391052>

723 Michaels, A.F., Caron, D.A., Swanberg, N.R., Howse, F.A., Michaels, C.M.,
725 1995. Planktonic sarcodines (Acantharia, Radiolaria, Foraminifera) in sur-
726 face waters near Bermuda: abundance, biomass and vertical flux. Journal of
727 Plankton Research 17, 131–163. <https://doi.org/10.1093/plankt/17.1.131>

728 Michaels, A.F., Knap, A.H., 1996. Overview of the U.S. JGOFS Bermuda

- 729 Atlantic Time-series Study and the Hydrostation S program. Deep Sea
730 Research Part II: Topical Studies in Oceanography 43, 157–198. [https://doi.org/10.1016/0967-0645\(96\)00004-5](https://doi.org/10.1016/0967-0645(96)00004-5)
- 731 Nakamura, Y., Itagaki, H., Tuji, A., Shimode, S., Yamaguchi, A., Hidaka,
732 K., Ogiso-Tanaka, E., 2023. DNA metabarcoding focused on difficult-to-
733 culture protists: An effective approach to clarify biological interactions.
734 Environmental Microbiology 25, 3630–3638. <https://doi.org/10.1111/1462-2920.16524>
- 735 Nakamura, Y., Suzuki, N., 2015. **Phaeodaria: Diverse marine cercozoans of**
736 **world-wide distribution.** Springer, pp. 223–249.
- 737 Ohman, M.D., 2019. A sea of tentacles: optically discernible traits resolved from
738 planktonic organisms in situ. ICES Journal of Marine Science 76, 1959–1972.
739 <https://doi.org/10.1093/icesjms/fsz184>
- 740 Panaïotis, T., Babin, M., Biard, T., Carlotti, F., Coppola, L., Guidi, L., Hauss,
741 H., Karp-Boss, L., Kiko, R., Lombard, F., McDonnell, A.M.P., Picheral, M.,
742 Rogge, A., Waite, A.M., Stemmann, L., Irisson, J.-O., 2023. Three major
743 mesoplanktonic communities resolved by in situ imaging in the upper 500
744 m of the global ocean. Global Ecology and Biogeography 32, 1991–2005.
745 <https://doi.org/10.1111/geb.13741>
- 746 Picheral, M., Guidi, L., Stemmann, L., Karl, D.M., Iddaoud, G., Gorsky, G.,
747 2010. The Underwater Vision Profiler 5: An advanced instrument for high
748 spatial resolution studies of particle size spectra and zooplankton. Limnology
749 and Oceanography: Methods 8, 462–473. <https://doi.org/10.4319/lom.2010.8.462>

- 752 8.462
- 753 Sogawa, S., Nakamura, Y., Nagai, S., Nishi, N., Hidaka, K., Shimizu, Y., Setou,
754 T., 2022. DNA metabarcoding reveals vertical variation and hidden diversity
755 of alveolata and rhizaria communities in the western north pacific. Deep
756 Sea Research Part I: Oceanographic Research Papers 183, 103765. <https://doi.org/10.1016/j.dsr.2022.103765>
- 757
- 758 Stukel, M.R., Biard, T., Krause, J., Ohman, M.D., 2018. Large Phaeodaria in
759 the twilight zone: Their role in the carbon cycle. Limnology and Oceanog-
760 raphy 63, 2579–2594. <https://doi.org/10.1002/lno.10961>
- 761 Stukel, M.R., Ohman, M.D., Kelly, T.B., Biard, T., 2019. The roles of
762 suspension-feeding and flux-feeding zooplankton as gatekeepers of particle
763 flux into the mesopelagic ocean in the northeast pacific. Frontiers in Marine
764 Science 6.
- 765 Suzuki, N., Not, F., 2015. Biology and ecology of radiolaria. Springer, pp.
766 179–222.
- 767 Swanberg, N.R., Anderson, O.R., 1981. Collozoum caudatum sp. nov.: A
768 giant colonial radiolarian from equatorial and Gulf Stream waters. Deep
769 Sea Research Part A. Oceanographic Research Papers 28, 1033–1047. [https://doi.org/10.1016/0198-0149\(81\)90016-9](https://doi.org/10.1016/0198-0149(81)90016-9)
- 770
- 771 Takahashi, K., Hurd, D.C., Honjo, S., 1983. Phaeodarian skeletons: Their role
772 in silica transport to the deep sea. Science 222, 616–618. <https://doi.org/10.1126/science.222.4624.616>
- 773
- 774 Whitmore, B.M., Ohman, M.D., 2021. Zooglider-measured association of zoo-

775 plankton with the fine-scale vertical prey field. Limnology and Oceanography
776 66, 3811–3827. <https://doi.org/10.1002/lno.11920>

777 Wood, S.N., 2017. Generalized additive models: an introduction with R, Second
778 edition. ed, Texts in statistical science. CRC Press/Taylor & Francis Group,
779 Boca Raton London New York.

780 Wood, S.N., 2001. mgcv: GAMs and Generalized Ridge Regression for R 1.

781 Zasko, D.N., Rusanov, I.I., 2005. Vertical Distribution of Radiolarians and
782 Their Role in Epipelagic Communities of the East Pacific Rise and the Gulf
783 of California. Biology Bulletin 32, 279–287. <https://doi.org/10.1007/s10525-005-0103-5>

784